Liu JL, Zhu S, Xu YL and Zhang Y (2011) Displacement-based design approach for highway bridges with SMA isolators. *Smart Structures and Systems*. 8(2): 173-190.

Displacement-based design approach for highway bridges with SMA isolators

Jin-long Liu[1,2], Songye Zhu[*1], You-lin Xu[1] and Yunfeng Zhang[3]

[1]*Department of Civil and Structural Engineering, The Hong Kong Polytechnic University, Hung Hom, Kowloon, Hong Kong, China*

[2]*Institute of Engineering Mechanics, China Earthquake Administration, Harbin 150080, China*

[3]*Department of Civil and Environmental Engineering, University of Maryland, College Park, MD, USA*

Abstract: As a practical and effective seismic resisting technology, the base isolation system has seen extensive applications in buildings and bridges. However, a few problems associated with conventional lead-rubber bearing have been identified after historical strong earthquakes, e.g. excessive permanent deformations of bearings and potential unseating of bridge decks. Recently the applications of shape memory alloys (SMA) have received growing interest in the area of seismic response mitigation. As a result, a variety of SMA-based base isolators have been developed. These novel isolators often lead to minimal permanent deformations due to the self-centering feature of SMA materials.

However, a rational design approach is still missing because of the fact that conventional design method cannot be directly applied to these novel devices. In light of this limitation, a displacement-based design approach for highway bridges with SMA isolators is proposed in this paper. Nonlinear response spectra, derived from typical hysteretic models for SMA, are employed in the design procedure. SMA isolators and bridge piers are designed according to the prescribed performance objectives. A prototype reinforced concrete (RC) highway bridge is designed using the proposed design approach. Nonlinear dynamic analyses for different seismic intensity levels are carried out using a computer program called "OpenSees". The efficacy of the displacement-based design approach is validated by numerical simulations. Results indicate that a properly designed RC highway bridge with novel SMA isolators may achieve minor damage and minimal residual deformations under frequent and rare earthquakes. Nonlinear static analysis is also carried out to investigate the failure mechanism and the self-centering ability of the designed highway bridge.

Keywords: Displacement-based design, shape memory alloy, base isolation, self-centering seismic resisting system, highway bridges, nonlinear response spectra

[*] Corresponding author, Assistant Professor, Email: ceszhu@polyu.edu.hk

1. Introduction

A large number of highway bridges have been damaged during the recent severe earthquakes, e.g. the Loma Prieta earthquake, the Kobe earthquake, the Chi-Chi earthquake and the Wenchan earthquake (Jankowski, *et al.* 1998, Chang, *et al.* 2000, Han, *et al.* 2009). The damaged and collapsed bridges not only lead to considerable economic and life losses, but also significantly delay the post-hazard rescue operation. Bridge's base isolators, generally installed between bridge decks and piers, have seen growing application in the last two decades. They are seen as an effective strategy for seismic hazard mitigation, and examples of these isolation devices include elastomeric bearings, lead rubber bearings (LRB) and frictional/sliding bearings (Dolce, *et al*. 2007, Hameed *et al*. 2008).

Although these isolators can protect structures from severe damages induced by strong ground motions, a large residual deformation is often inevitable. As pointed out by Piestley (1997) and Kwan and Billington (2003), the residual displacements are likely more important than the maximum displacements when the difficulty of repair after earthquakes is considered. In light of the emphasis on the residual displacements, a series of self-centering seismic resistant structures have been developed (Kwan and Billington 2003, Christopoulos *et al*. 2002). They are often associated with minimal residual deformation after an earthquake, even if considerably inelastic transient deformations arise during seismic response. Among various self-centering schemes, the utilization of the superelasticity feature SMA devices on bridges has attracted growing research interest (Wilson and Wesolowsky 2005; Song *et al.* 2006). For example, Andrawes and DesRoches (2005) and Zhang *et al.* (2008, 2009) studied the effectiveness of superelastic SMA devices for the reduction of seismic response of bridges. Graesser and Cozzarelli (1991) suggested the use of Nitinol (Nickel Titanium Naval Ordnance Laboratory) as seismic isolations, and proposed a one-dimensional constitutive model for the superelastic behavior of SMA. Wilde *et al* (2000) carried out a numerical study of a smart isolation system which combines a laminated rubber bearing with a SMA-made device to control the seismic response of highway bridges, and they reported that under small and medium ground excitations, the relative displacement between deck and pier was decreased obviously at the expense of a larger shear force on piers. Choi *et al.* (2005) added the superelastic Nitinol wires into a bridge's base isolation system, and the residual deformation was effectively controlled. Dolce *et al.* (2007) have incorporated the superelastic Nitinol wires in

elastomeric bearings to provide re-centering and/or additional energy dissipating capability for a bridge's base isolation system, and the benefits to control structural and non-structural damage were validated by shaking table tests of isolated RC frames. Casciati and Faravelli (2009) and Casciati *et al.* (2007) proposed a novel base isolation device composed of SMA bars with a larger amount of energy dissipation, and the analytical study by Casciati *et al.* (2009) indicated that the novel SMA isolators can effectively reduce the displacement response of a highway bridge during strong earthquakes.

Although the promise of SMA base isolators for highway bridges has been analytically and experimentally demonstrated through the aforementioned studies, a rational design approach is still missing for highway bridges with these novel devices. The conventional design method for common base isolators cannot be directly applied to these novel devices, as the strength, stiffness and hysteretic behavior is greatly different. In light of this limitation, an extension of the displacement-based design (DBD) procedure for highway bridges supported on SMA isolators is presented in this paper. It should be noted that DBD has been recognized as a more rational design approach in the framework of performance based earthquake engineering, in comparison with conventional force-based design method (Kowalsky, *et al*. 1995. Priestley 1997, Priestley and Kowalsky 2000, Medhekar and Kennedy 2000, Chopra and Goel 2000, Chopra and Goel 2001, Kowalsky 2002 and Lin, *et al.* 2003). The standard DBD is extended in this study to design self-centering highway bridges with novel SMA isolators. Nonlinear response spectra, derived from typical hysteretic models for SMA materials, are employed in this procedure. The design performance objectives are prescribed first for the SMA isolators and bridge piers. A prototype of a RC highway bridge is designed based on the proposed design approach. Seismic performances of the designed highway bridge, including the failure mechanism and re-centering ability, are investigated through nonlinear dynamic analyses at two seismic intensity levels – frequent and rare earthquakes. The efficacy of the DBD approach is validated by numerical simulations. Furthermore, the high performance RC bridge with novel SMA isolators designed according to the proposed approach experiences only minor damage and minimal residual displacement under frequent and rare earthquakes.

2. SIMPLIFIED MODELING

2.1 Constitutive model of superelastic SMA

SMA refers to one type of unique alloys which is able to return to its undeformed state by shape memory effect or superelastic effect. The former one refers to the phenomenon that at ambient temperature T<M_f, the residual deformation after unloading can be fully recovered through a temperature increase; while the latter one arises at ambient temperature T>A_f, in which SMA immediately recovers to original shape with almost zero residual strain upon unloading. Here M_f and A_f denote the martensite and austenite finish temperatures respectively. Nitinol alloy, as most practical SMA, has been studied for use as seismic damping devices due to its inherent self-centering capability, high ductility, good corrosion resistance and long fatigue life. Fox example, the maximum recoverable strain of superelastic Nitinol wires can reach up to 8%, and they can sustain over 2,000 load cycles under 8% strain cycles (Zhu and Zhang, 2008). In this study, the superelasticity of Nitinol will be utilized to realize the self-centering behavior.

A one-dimensional flag-shaped constitutive model is used to describe the superelastic behavior of Nitinol. The model is defined by six parameters – austenite elastic modulus E_A, martensite elastic modulus E_M, phase-transformation modulus ratio α (i.e. 'post-yield' stiffness ratio), phase transformation start stress σ_y (i.e. 'yield' stress), phase transformation finish strain ε_M and energy dissipation coefficient β (as shown in Fig. 1). The parameters are tuned according to the stress-strain relationship of Nitinol wires produced by Johnson Matthey Inc. (2010) when cyclically tested at the frequency of 2Hz:

$$E_A = 39 \text{ GPa}, E_M = 19 \text{ GPa}, \sigma_y = 390 \text{ MPa}, \alpha = 0.036, \varepsilon_M = 0.062, \beta = 0.4$$

An apparent strain hardening can be observed at large strain, to which attention should be paid because of the potential overloading to adjacent members. The fracture strain of Nitinol wires is over 14%. According to (Zhang and Zhu, 2008), although the flag-shaped constitutive model could not accurately simulate the unloading path, and does not reflect the loading rate effect, it can predict the seismic response with satisfactory accuracy with regard to peak displacements, accelerations and ductility ratios in both SDOF

systems and MDOF systems, as far as its parameters are tuned to dynamic test data.

To enable the dynamic analysis of highway bridges with SMA devices, this constitutive model has been implemented in the computer program OpenSees (Mazzoni *et al.* 2006) as a new material model.

2.2 SMA base isolator

A few SMA-based isolation systems have been developed and investigated by different researchers (Wilde, *et al*. 2000, Choi, *et al*. 2005, Dolce *et al*. 2007, Casciati *et al*. 2007). A common feature of these isolators is self-centering (also called re-centering) capability due to the superelastic behavior of Nitinol alloys or other SMAs. Fig. 2(a) shows a scheme of a highway bridge isolation system, in which SMA elements are used together with elastomeric bearings (or sliding bearings). The lateral stiffness and capacity of elastomeric bearings are often much smaller than those of SMA elements (Wilde, *et al*. 2000). Therefore the elastomeric bearings are treated as gravity load transfer elements in this study, while the lateral seismic load resistance is mainly offered by SMA cables. The SMA cables are assumed to undertake tensile force only. It should be noted that the schematic drawing shows a general model of some common SMA base isolators, and it may not necessarily be a real configuration to be implemented in real bridges. The DBD approach presented in this study can be easily adapted to aforementioned SMA isolators with similar hysteresis. Although only the longitudinal SMA cables are shown in Fig. 2(a), similar elements should also be arranged in transversal direction in real bridges.

2.3 Equivalent SDOF system of a highway bridge with SMA isolators

In DBD approach, it is assumed that seismic response of structures is often dominated by the fundamental vibration mode so that it can be modelled by an equivalent SDOF system. Fig. 2(b) shows a simplified model of the highway bridge with isolators, where k_p, k_b and k_s represent the stiffness of the bridge pier, elastomeric

bearing and SMA isolator respectively. As mentioned before, the spring k_b only provides vertical stiffness, and their contribution to the overall lateral stiffness of the bridge is neglected. Therefore, the bridge can be further simplified as an equivalent nonlinear SDOF system shown in Fig. 2(c) when subject to horizontal ground motions in longitudinal direction, where u_1 and u_2 stand for the longitudinal displacement at the deck level and the pier top level respectively, $f_{12}(t)$ represent the seismic force applied on the deck, and m is seismic tributary mass to each bridge pier. The total mass of the superstructure is concentrated at deck level, and the mass of the pier is not considered in the design process according to the study by Turkington *et al* (1989a, 1989b). The isolators between bridge piers and decks are often used to protect the concrete piers from significant damage. Therefore it is always desirable to design the capacity of the bridge piers higher than the 'yield load' of the SMA isolators. Consequently, the system shown in Fig. 2(c) can be approximated by a nearly linear spring in series with a nonlinear spring with flag-shaped hysteresis. As shown in Fig. 3(c), the consequent hysteresis is still in a flag shape, however, the stiffness and ductility of the equivalent system is different from those of the SMA materials. Easy to know that the yield displacement and the maximum displacement of the equivalent system is

$$u_{eq}^{y} = u_{s}^{y} + u_{p}^{y} \tag{1}$$

$$u_{eq}^{m} = u_{s}^{m} + u_{p}^{m} \tag{2}$$

where u_{eq}^{y}, u_{s}^{y}, u_{p}^{y} are, respectively, the yield displacement of the system, the yield displacement of the SMA isolator, and the top displacement of the pier corresponding to the yielding of the isolators; while $u_{eq}^{m}, u_{s}^{m}, u_{p}^{m}$ is the maximum displacement of equivalent system, SMA isolator, and the top of the bridge pier. The elastic stiffness and the post-yield stiffness ratio of the SMA isolator are k_s and α, and its ductility is defined as

$$\mu = \frac{u_{s}^{m}}{u_{s}^{y}} \tag{3}$$

Therefore the ductility, elastic stiffness and post-yield stiffness ratio of the equivalent system can be computed as follows

$$\mu_{eq} = \frac{u_{eq}^m}{u_{eq}^y} = \frac{u_s^m + u_p^m}{u_s^y + u_p^y} \tag{4}$$

$$k_{eq} = \frac{k_s k_p}{k_p + k_s} \tag{5}$$

$$\alpha_{eq} = \frac{\alpha k_s k_p}{(\alpha k_s + k_p) k_{eq}} = \frac{\alpha(1 + k_s / k_p)}{(\alpha k_s / k_p + 1)} \tag{6}$$

μ_{eq}, k_{eq} and α_{eq} are not equal to μ, k_s and α unless k_p is infinite.

2.4 Nonlinear SDOF response spectra

It is well known that the seismic response of the structures is substantially dependent on the nonlinear hysteretic behavior. Nonlinear response spectra of SDOF system with various hysteretic models have been extensively studied (Newmark and Hall 1982, Nassar and Krawinkler 1991, Vidic, et al. 1994, Seo and Sause 1995). This section studies the nonlinear response spectra of SDOF system, in which a flag-shaped hysteresis showing strain hardening at large strain is used. The hysteretic model is described in Fig. 3. The derived nonlinear response spectra will be employed in DBD approach presented in the next section. Three major parameters are considered in the nonlinear response spectra, namely the initial period T_0 (from 0.2 to 3 seconds), the post-yield stiffness α ($= 0, 0.1, 0.2, 0.3, 0.4$) and the strength reduction factor R (=1,2,3,4,5,6,7,8). T_0 and R could be calculated by

$$T_0 = 2\pi\sqrt{m / k_{eq}} \tag{7}$$

$$R = F_e / F_y \tag{8}$$

where k_{eq} is the initial stiffness of the SDOF system, F_e is the elastic design strength and F_y is the 'yield' strength of the equivalent nonlinear system.

A ground motion suite containing a total of 20 earthquake records, designated as EQ01-EQ20, is employed in the computation. These 20 ground motions were derived from ten earthquakes, each comprising two perpendicular components. They are scaled to match the seismic design spectrum of rare earthquake level for seismic intensity level of 7.5 and site class II specified in Chinese seismic design code (2001) using the scaling method proposed by Zhu and Gao (2009). Fig. 4 shows the design spectrum, and the response spectra of the 20 scaled records. It is seen that the median spectrum can well match the design spectrum within the period range of interest.

Fig. 5 shows the median spectra of ductility response, for varying parameters T_0, α and R. Seo (2005) emphasized the median response as the likely response for a set of ground motions based on the assumption that nonlinear response follows a lognormal distribution. Furthermore, Seo (2005) proposed a regression function to fit the nonlinear μ-R-T_0 relationship of SDOF system for different types of hysteresis:

$$\mu_{eq}(T_0, R, \alpha) = R^{\exp(c1/T_0^{c2})} \tag{9}$$

where μ_{eq} is the regression value of ductility, T_0 is the initial period, R is the strength reduction factor, c_1 and c_2 are functions of post-yield stiffness ratio α, with

$$c_1(\alpha) = (a - b\sqrt{\alpha})^2 \quad , \quad c_2(\alpha) = (c - d\sqrt{\alpha})^2 \tag{10}$$

It can be seen that the relationship is characterized by four parameters a, b, c, d. This regression function is also adopted in this study to simulate the nonlinear response spectra corresponding to hysteretic behavior of SMA. Through regression analysis, the four parameters in this paper are taken as a = 0.408, b= 0.904, c = 0.98, d = -0.37. The simulation results of the nonlinear response spectra are also shown in Fig. 5. It can be seen that the regression function can well match the median spectra of the ductility over the period range of interest. Consequently the force reduction factor can be expressed as

$$R(T_0, \mu_{eq}, \alpha) = \mu_{eq}^{\exp(-c1/T_0^{c2})} \tag{11}$$

3. DBD approach

DBD approach has been developed and applied by some researchers to the seismic design of different structures (Kowalsky, *et al*. 1995, Kowalsky 2002, Priestley 1997, Priestley and Kowalsky 2000, Lin *et al*. 2003, Medhekar and Kennedy 2000). In conventional DBD approach, nonlinear structure systems are usually modeled by an equivalent linear system with equivalent elastic stiffness and equivalent viscous damping. Chopra and Goel (2000, 2001) revised this approach by incorporating nonlinear design spectra in order to improve the accuracy of the performance prediction. In this study, the DBD approach using nonlinear design spectra is further extended to the design of highway bridges with SMA base isolators. The objective is to design a highway bridge with SMA isolators in order to achieve the target performance level under given intensity of ground motions, e.g. the maximum displacement, ductility and damage extent. The following assumptions are made within the DBD procedure: the vibration of the isolated highway bridge is dominated by the first mode and the mode shape is maintained during the earthquake; the lateral strength of the piers are higher than the yield load of the SMA isolators so that the seismic behavior of the piers is almost linear; the mass of the pier is relative small and can be ignored in comparison with that of the deck; all piers of the highway bridge have the same height. As the elastomeric bearing provides only gravity carrying capacity, its design is not discussed hereinafter. The design procedure is elaborated as follows:

Step one: Target Seismic Performance

Once basic structural parameters (e.g. mass and height) are known, the target performance levels under design earthquake level should be determined, including the peak displacement at the top of the pier u_p^m, the relative displacement between the deck and the pier u_s^m, and the maximum ductility of SMA elements μ. The first one u_p^m determines the damage level of the bridge pier. In order to prevent the bridge pier from significant damage and noticeable residual deformation after an earthquake, it is desirable to limit its drift

ratio to the elastic limit state.

The peak relative displacement u_s^m should be determined by taking into account various factors such as the impact between the deck and the abutment, the potential unseating of bridge decks, the damage of joint connections and the deformation capacity of elastomeric bearings. According to Zhang and Zhu (2008), SMA cannot be fully recovered to its original shape after being loaded beyond 8% of strain, and thus partially loses its self-centering capability. Therefore the ductility level of SMA has to be limited if minimal residual displacement after an earthquake is desired.

Step two: Equivalent SDOF System

The peak displacement of the bridge deck can be easily estimated from Eq. (2). The restoring forces of SMA base isolators can be calculated by

$$F_s^y = k_s u_s^y \tag{12}$$

$$F_s^m = k_s u_s^y + \alpha k_s (\mu - 1) u_s^y \tag{13}$$

where F_s^y and F_s^m are respectively the yield force and peak forces of the isolators respectively. Meanwhile, the piers are in elastic state under considered seismic level. As the piers are in series with the SMA isolators, the resisting forces are always equal in these two elements.

$$F_s^y = k_p u_p^y \tag{14}$$

$$F_s^m = k_p u_p^m \tag{15}$$

Therefore, the ratio of the lateral stiffness $\eta = k_s / k_p$ can be calculated from Eqs (12)–(15). The ductility μ_{eq} and the post yield stiffness ratio α_{eq} of the simplified equivalent SDOF system can be subsequently computed by

$$\mu_{eq} = u_{eq}^m / [u_s^y (1 + \eta)] \tag{16}$$

$$\alpha_{eq} = \alpha(1 + \eta) / (1 + \alpha\eta) \tag{17}$$

Step three: Nonlinear Design Spectrum

The elastic design spectra (including pseudo acceleration spectrum S_{ae} and displacement spectrum S_{de}) can be obtained from the design code. The nonlinear acceleration spectra S_a and the displacement spectra S_d can be constructed by

$$S_a(T_0, \mu_{eq}, \alpha_{eq}) = S_{ae} / R \tag{18}$$

$$S_d(T_0, \mu_{eq}, \alpha_{eq}) = \mu_{eq} S_{de} / R \tag{19}$$

where μ_{eq} and α_{eq} are calculated from Eq. (16) and (17). Based on the target displacement of the bridge deck u_{eq}^m, the initial period T_0 and the corresponding acceleration level S_a can be easily determined according to Fig. 6.

Step four: Design of Isolators and Bridge Piers

The yield load of the bridge isolator is equal to

$$F_s^y = m \cdot S_a \tag{20}$$

The lateral stiffness of the equivalent SDOF system, the SMA isolator and the bridge pier can be computed by

$$k_{eq} = 4\pi^2 m / T_0^2 \tag{21}$$

$$k_p = k_{eq}(1+\eta)/\eta \tag{22}$$

$$k_s = \eta k_p \tag{23}$$

Once the yield load, initial stiffness, peak deformation and ductility level of the isolators are determined, the length and cross sectional area of the SMA elements can be computed. Subsequently, with the desired stiffness and strength of the bridge piers, the cross section of RC piers can be designed. In order to protect the pier from significant damage, the bridge pier is typically designed to have a greater lateral strength than the yield load of the SMA isolators.

Step five: Check Seismic Performance

The seismic performance levels of the designed highway bridge needs to be checked through nonlinear static analyses and time-history analyses, particularly under other seismic intensity levels that are not considered in the design procedure.

4. Case study

4.1 Design example

The example consists of a four-span RC highway bridge with three six-meter high piers and two rigid abutments, as shown in Fig. 7. The bridge has four 20 m continuous spans, and the width of deck is 12 m. The total mass of the superstructure is about 2000 ton. All the piers and the deck are reinforced concrete members. The material properties of SMA are shown in section 2.1. According to the Chinese seismic design code (2001), the bridge is designed for site class II and intensity level 7.5 with the peak ground acceleration of 0.31g (rare earthquake). The site classification in Chinese seismic design code is presented in Table 1. The corresponding elastic design spectrum is shown in Fig. 4. The objective is to design the highway bridge with target peak displacements and minimal residual deformation under the considered seismic intensity level. The peak drift ratio of the piers is taken as 1/600 (i.e. u_p^m=1cm), and the ductility of SMA elements are taken as μ=6. The peak displacement of the bridge deck is selected to be 12 cm based on the study by other researchers on highway bridges (Choi, *et al*. 2005, Dolce, *et al*. 2007). Using the above-described design procedure, the following structural parameters are determined: the length of SMA element $l_0 = 183$cm; the cross-sectional area of the SMA element in each isolator A=11.3 cm^2; the effective width and height of the cross-section of the pier b=1.8 m and h=1.1 m; a total of 18 steel bars with 25 mm diameter arranged along the width (one side) of each pier.

In order to assess the efficacy of the proposed DBD approach, a finite element model of the designed bridge is built using the computer program OpenSees (Mazzoni *et al.* 2006). The new material's model is developed

in OpenSees to simulate the superelastic behavior of SMA. The pier and the deck are all simulated by nonlinear beam-column elements with fiber sections. Nonlinear static analysis (i.e. pushover analysis) and nonlinear time-history analyses are carried out in order to evaluate the seismic performance of the designed highway bridge under different seismic intensity levels. Only the seismic ground motions in longitudinal direction are considered.

4.2 Pushover analysis of the pier

A pushover analysis as defined by *NEHRP recommendation provisions for seismic regulations for new buildings and other structures* (FEMA 450) (2003) is carried out to evaluate the failure mechanism and self-centering capability of the isolated highway bridge. The pushover curves are shown in Fig. 8. Fig. 8(a) illustrates the relationship between the total base shear of three piers and the deck displacement, in particular, two unloading paths corresponding to medium deformation and large deformation of the SMA isolators are indicated. The corresponding force-displacement relationship of the piers and SMA isolators are shown in Fig. 8(b). It is seen that the concrete piers crack at relative small displacement (point 1), and it results in a slight reduction in the lateral stiffness of the bridge piers. Point 2 stands for the 'yield' load of the isolators, which is actually due to stress-induced phase transformation of SMA instead of conventional yield mechanism. It should be noted that the yield strength of the piers (point 4) is designed to have higher yield strength than the yield load of the SMA isolators in order to effectively protect the piers from significant damage. Therefore the pier behavior is nearly linear elastic when the isolator yields. As a result, the residual deformation of the highway bridge will be ignorable when unloaded from the yield plateau (as shown by the unloading path *a*). Point 3 represents the end of phase transformation, and obvious strain hardening can be observed after point 3. The slope of the curve is governed by the modulus of elasticity of martensite SMA. The stain hardening behavior of the SMA isolators results in a larger force exerted on the bridge piers. Consequently, the steel

reinforcement in the bridge pier begins to yield at point 4, and the system reaches its maximum capacity. Further loading beyond point 4 leads to noticeable plastic deformation in the bridge piers. As shown by the unloading path *b*, an apparent residual displacement can be observed in the bridge piers, even though the SMA isolators can still recover their deformation, and the self-centering capability is partially lost. Therefore, if the peak response is below point 1, there is no crack in concrete piers, both the bridge's piers and isolators behaves linearly, and the whole highway bridge is almost damage free; from point 1 to 4, the highway bridge is only subjected to minor damage in the bridge piers without yielding of steel reinforcement and noticeable residual displacement. This feature will considerably reduce the post-earthquake repair cost. However, relatively large damage of the bridge pier may result from the strain hardening behavior of SMA at large strain. It implies that neglecting the strain hardening behavior in the constitutive model of SMA may lead to an underestimation of pier's damage in seismic analyses.

4.3 Nonlinear dynamic analyses

—The aforementioned twenty earthquake records are employed to investigate the actual seismic response of the designed highway bridge. Following Chinese seismic design code (2001), the twenty ground motions are scaled to match the design spectra of rare earthquakes (2-3% exceedance probability in 50 years) and frequent earthquakes (63% exceedance probability in 50 years) respectively.

Figures 9-13 show the seismic response under the 20 rare earthquake records. The median values of the peak displacements for the bridge pier, SMA isolators, and the bridge deck are 0.9 cm, 10.3 cm and 11.6 cm respectively, which are close to the target displacements specified in the design procedure, namely 1.0 cm, 11.0 cm and 12.0 cm. The median ductility of SMA elements, i.e. 5.6, is close to the target value μ=6 as well. In general, the proposed DBD approach is able to fairly well achieve the target displacement and ductility specified in the design procedure.

Fig. 10 shows the peak and residual displacements of the bridge pier for all 20 rare earthquake records. Although the concrete piers tend to crack in all rare earthquakes, the bridge piers do not reach their yield strength under 18 earthquake records. Furthermore, the residual displacement of the highway bridge is ignorable under all the rare earthquakes except for EQ15. This clearly manifests the merit of the self-centering feature of the SMA isolators. The limited damage in the bridge piers, together with nearly zero residual drift ratios will considerably reduce the post-earthquake repair cost and effort. The results imply that highway bridges with SMA isolators, if properly designed, are able to achieve a high seismic performance in comparison with conventional bridge systems. The peak displacement is maximum under EQ15 among all 20 ground motions. The SMA isolators under EQ15 enter into the martensite range, and the strain hardening of SMA at large deformation leads to an increased base shear. As a result, the bridge piers yield during EQ15, and the plastic deformation of the bridge piers causes noticeable residual displacement after the earthquake. These dynamic analysis results further justify the necessity of properly modeling the strain hardening at large strain in the constitutive model of SMA. Figures 11-13 show the displacement time history of the pier, and the force-displacement relationship of the piers and SMA isolators under EQ01 and EQ15. They provide further supports to the above statements.

Fig. 14 shows the peak and residual displacements of the bridge pier under 20 frequent earthquake records. The median value of the peak displacement is about 0.46 cm. No yielding of steel reinforcement occurs under all the 20 records, and the bridge piers behave almost linearly. Consequently no apparent residual displacement is observed after all the earthquakes. In around 15 earthquakes, the peak response of the bridge is below point 1 shown in Figure 8, and the highway bridge is almost damage free without any cracks in the bridge piers. The highway bridge is therefore associated with minor damages or even no damage after frequent earthquakes.

5. Conclusion

In this paper, a displacement-based seismic design procedure for highway bridges supported on SMA isolators is presented. Nonlinear response spectra derived from the constitutive model for SMA materials is employed in the design procedure. A simplified SDOF model consisting of two springs in series is used to represent the highway bridge. A four-span RC highway bridge is designed using the proposed design approach, in which the major parameters of the bridge piers and SMA isolators are determined based on the desired seismic performance objectives, including the target drift ratio of the bridge piers, target displacement of the bridge deck and the target ductility of the SMA isolators.

A finite element model of the design example is built in OpenSees computer program. Nonlinear static and time-history analyses are carried out to investigate its actual seismic behavior. The results indicate that the simplified model can well predict the seismic response of the highway bridges of interest, and the proposed DBD procedure can well achieve the target performance specified in the design procedure. Furthermore, the highway bridges supported on SMA isolators, if properly designed, are associated with minor damage under rare earthquakes, and are likely damage free under frequent earthquakes. The residual deformations after earthquakes are minimal due to the superior self-centering feature of the SMA isolators. The high seismic performance will considerably reduce the post-earthquake repair cost and the corresponding downtime. In addition, both nonlinear static and dynamic analyses indicate that neglecting the strain hardening in the constitutive model of SMA may result in an underestimation of seismic damage in the bridge's piers.

It should be noted that the bridge piers are assumed to be of the same height, and the effect of vertical ground motions are not considered in this study. Further development of this design procedure is needed in future to appropriately address these two issues.

Acknowledgement

The authors are grateful for the financial support from The Hong Kong Polytechnic University through research grant (PolyU-1-87SZ and PolyU-A-PJ15). Findings and opinions expressed here, however, are those of the authors alone, not necessarily the views of the sponsoring agencies.

References

Andrawes B., and DesRoches R. (2005), "Unseating prevention for multiple frame bridges using superelastic devices", *Smart Materials and Structures*, 14:S60-S67.

Casciati F., and Faravelli L. (2009), "A passive control device with SMA components: from the prototype to the model", *Structural Control and Health Monitoring*, 16: 751-765.

Casciati F., Faravelli L., and Hamdaoui K. (2007), "Performance of a base isolator with shape memory alloy bars", *Earthquake Engineering and Engineering Vibration*, 6(4):401-408.

Casciati F., Faravelli L. and Al Saleh R. (2009), "An SMA passive device proposed within the highway bridge benchmark", *Structural Control and Health Monitoring*, 16(6): 657-667.

Chang K.C., Chang D.W., Tsai M.H. and Sun Y.C. (2000), "Seismic performance of highway bridges", *Earthquake Engineering and Engineering Seismology*, 2(1):55-77.

Choi E., Nam T.H., and Cho B.S. (2005), "A new concept of isolation bearings for highway steel bridges using shape memory alloys", Can. J. Civ. Eng., 32(5): 957-967.

Chopra A.K., and Goel R.K. (2000), "Evaluation of a NSP to estimate seismic deformation: SDF system", *Journal of Structural Engineering (ASCE)*, 126(4):482-490.

Chopra A.K., and Goel R.K. (2001), "Direct displacement-based design: use of inelastic vs. elastic design spectra", *Earthquake Spectra*, 17(1):47-64.

Christopoulos C., Filiatrault A., and Folz B. (2002), "Seismic response of self-centering hysteretic SDOF systems", *Earthquake Engineering and Structural Dynamics*, 31:1131-1150.

Dolce, M., Cardone, D. and Palermo G. (2007), "Seismic isolation of bridges using isolation systems based on flat sliding bearings", *Bull Earthquake Eng*, 5:491-509

Graesser E.J., and Cozzarelli F.A. (1991), "Shape memory alloys as new materials for aseismic isolation", *Journal of Engineering Mechanics (ASCE)*, 117(11):2590-2608.

Hameed A., Koo M.S., Dai Do T.D., and Jeong J.H. (2008), "Effect of lead rubber bearing characteristics on the response of seismic-isolated bridges", *KSCE Journal of Civil Engineering*, 12(3):187-196.

Han Q., Du X.L., Liu J.B., Li Z.X, Li L.Y. and Zhao J.F. (2009), "Seismic damage of highway bridges during the 2008 Wenchuan earthquake", *Earthquake Engineering and Engineering Vibration*, 8:263-273.

Jankowski, R., Wilde, K. and Fujino, Y. (1998), "Pounding of superstructure segments in isolated elevated bridge during earthquakes", *Earthquake Engineering and Structural Dynamics*, 27:487-502.

Johnson Matthey, Inc (2010) www.jmmedical.com

Kowalsky M.J., Priestley M.J.N., and MacRae G.A. (1995), "Displacement-based design of RC bridge columns in seismic regions", *Earthquake Engineering and Structural Dynamics*, 24(12):1623-1643.

Kowalsky M.J. (2002), "A displacement-based approach for the seismic design of continuous concrete bridges", *Earthquake Engineering and Structural Dynamics*, 31:719-747.

Kwan W.P., and Billington S.L. (2003), "Unbonded Posttensioned Concrete Bridge Piers. I: Monotonic and Cyclic Analyses", *Journal of Bridge Engineering (ASCE)*, 8(2):92-101.

Lin Y.Y., Tsai M.H., Hwang J.S., and Chang K.C. (2003), "Direct displacement-based for buildings with passive energy

dissipation systems", *Engineer Structures*, 25(1):25-37.

Mazzoni, S., McKenna, F., Scott, M.H., Fenves, G.L. (2006) Open system for earthquake simulation user command-language manual,, OpenSees version 1.7.3. Pacific Earthquake Engineering Research Center, University of California, Berkeley.

Medhekar M.S., and Kennedy D.J.L. (2000), "Displacement-based seismic design of buildings-theory", *Engineering Structures*, 22:201-209.

Medhekar M.S., and Kennedy D.J.L. (2000), "Displacement-based seismic design of buildings-application", *Engineering Structures*, 22:210-221.

Nassar A.A., and Krawinkler H. (1991), "Seismic damands for SDOF and MDOF systems", Rep. No 95, *John Blume Earthquake Engineering Center*, Department of Civil Engineering, Stanford University, CA

National standard of the People's Republic of China (2001). *Code for seismic design of buildings (GB 50011-2001)*. Beijing; [in Chinese].

Newmark, N.M., and Hall, W.J. (1982), *Earthquake spectra and design*, Earthquake Engineering Research Institute, Berkeley, Calif.

Priestley, M. J. N. (1997), "Displacement-based seismic assessment of reinforced concrete buildings", *Journal of Earthquake Engineering*, 1(1):157-192.

Priestley, M. J. N. (1997), "Myths and fallacies in earthquake engineering", *Concr. Int*., 19(2): 54-63.

Priestley M.J.N., and Kowasky M.J. (2000), "Direct displacement-based seismic of concrete buildings", *Bulletin of the New Zealand National Society for Earthquake Engineering*, 33(4):421-442.

Seo, C.Y. and Sause, R. (2005), "Ductility demands on self-centering systems under earthquake loading", *ACI Structural Journal*. 102(2): 275-285.

Seo C.Y. (2005), "Influence of ground motion characteristics and structural parameters on seismic response of SDOF systems", Ph.D dissertation, Lehigh University.

Song G., Ma N. and Li H. N. (2006), "Applications of shape memory alloys in civil structures," *Engineering Structures*, 28: 1266-1274.

Turkington D.H., Carr A.J., Cooke N., and Moss P.J. (1989a), "Seismic design of bridges on lead-rubber bearings", *Journal of Structural Engineering (ASCE)*, 115(12):3000-3016.

Turkington D.H., Carr A.J., Cooke N., and Moss P.J. (1989b), "Design method for bridges on lead-rubber bearings", *Journal of Structural Engineering (ASCE)*, 115(12):3017-3030.

U.S. building seismic safety council. (2003), *NEHRP recommendation provisions for seismic regulations for new buildings and other structures* (FEMA 450).

Vidic T., Fajfar P., and Fischinger M. (1994), "Consistent inelastic design spectra: strength and displacement", *Earthquake Engineering and Structural Dynamics*, 23:507-521.

Wilde W., Gardoni P., and Fujino Y. (2000), "Base isolation system with shape memory alloy device for elevated highway bridges", *Engineering Structures*, 20:222-229

Wilson J.C. and Wesolowsky M.J. (2005), "Shape memory alloys for seismic response modification: a state-of-the-art review", *Earthquake Spectra*, 21(2): 569-601.

Zhang Y.F., Camilleri J.A., and Zhu S.Y. (2008), "Mechanical properties of superelastic Cu-Al-Be wires at cold temperatures for the seismic protection of bridges", *Smart Materials and Structures*, 17, 025008 (9pp).

Zhang Y., Hu X. and Zhu S. (2009), "Seismic performance of benchmark base isolated bridges with superelastic Cu-Al-Be wire damper", *Structural Control and Health Monitoring*, 16(6): 668-685.

Zhang Y. and Zhu S. (2008), "Seismic resistant braced frame structures with shape memory alloy-based self-centering damping device". *In: Miura, T., Ikeda, Y. (eds.): Earthquake Engineering: New Research, Nova Science Publisher, Inc.,* Hauppauge, USA, 219-254.

Zhang, Y. and Zhu, S. (2008), "Seismic response control of building structures with superelastic Shape Memory Alloy wire damper", *Journal of Engineering Mechanics(ASCE)*, 134(3): 240-251.

Zhu, S. and Gao, Y. (2009), "Genetic algorithm-based development of ground motion time histories". Proceedings of 2009 ANCER Workshop, University of Illinois Urbana-Champaign, IL, USA, August 13-14.

Zhu S. and Zhang Y. (2008), "Seismic analysis of concentrically braced frame systems with self-centering friction damping braces", *Journal of Structural Engineering (ASCE)*, 134(1): 121-131.

Figure list

Table 1. Site class definition for seismic design (China's code for seismic design of buildings 2001)

Equivalent shear wave velocity (m/s)	Total thickness of overlaying layers for each class* (m)			
	I	II	III	IV
$v_{se} > 500$	0			
$500 \geq v_{se} > 250$	<5	≥5		
$250 \geq v_{se} > 140$	<3	3~50	>50	
$v_{se} \leq 140$	<3	3~15	15~80	>80

* the thickness of overlaying layer is the distance measured from ground to underlying rock layer (i.e. the layer with $v_{se} > 500$ m/s)

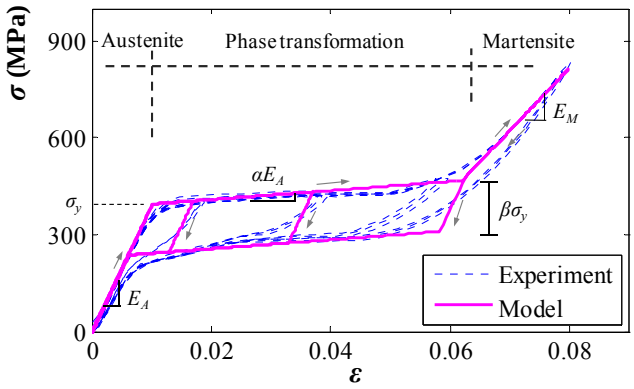

Fig. 1 Constitutive model of superelastic SMA

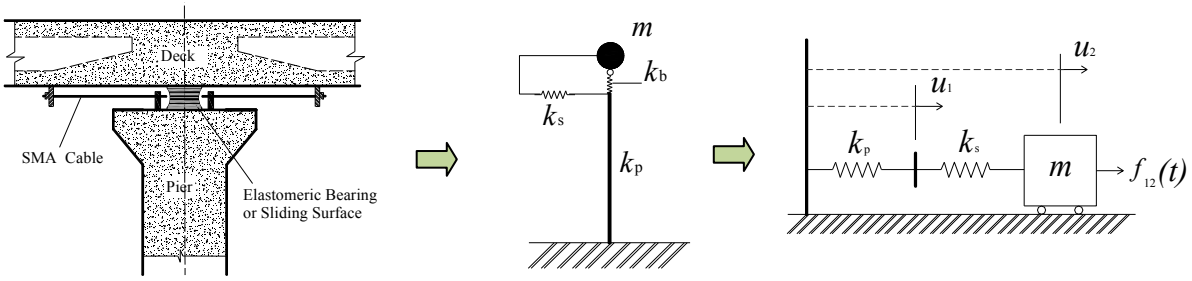

(a) Schematic configuration of a highway bridge isolators (b) modelling of an isolated highway bridge (c) simplified modelling

Fig. 2 Simplified modelling of a highway bridges with SMA base isolators

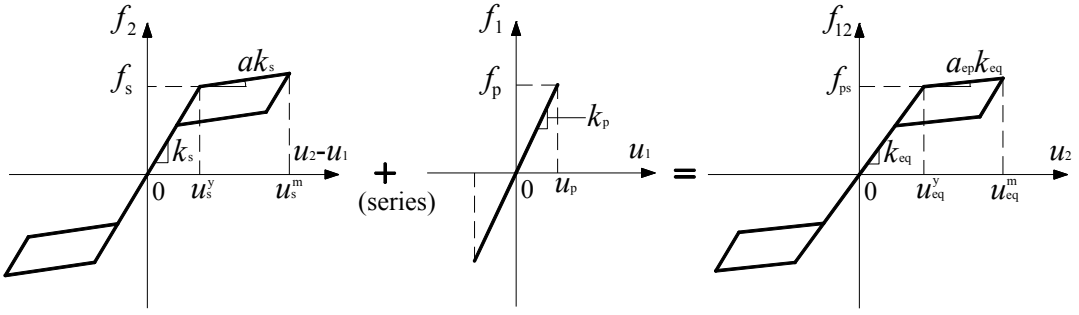

(a) SMA isolator (b) Bridge pier (c) Equivalent system

Fig. 3 Hysteretic behavior of the highway bridge with SMA isolators

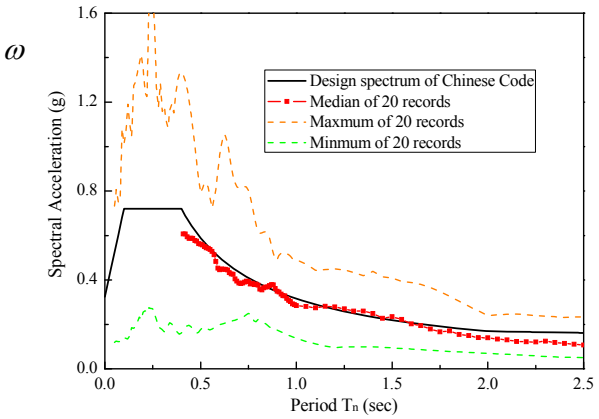

Fig. 4 Acceleration response spectra of 20 earthquake records considered

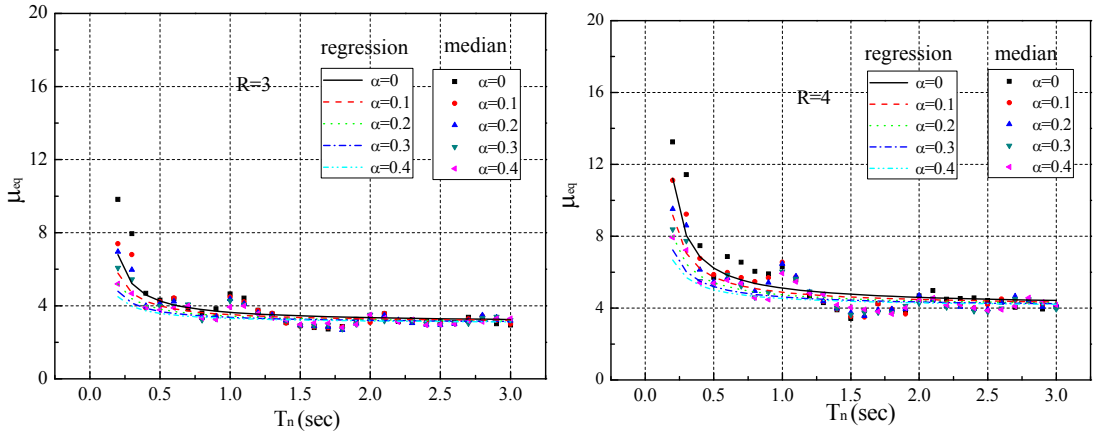

(a) R=3 (b) R=4

(c) R=5 (d) R=6

Fig. 5 The median spectra of the ductility μ_{eq} for varying R and α

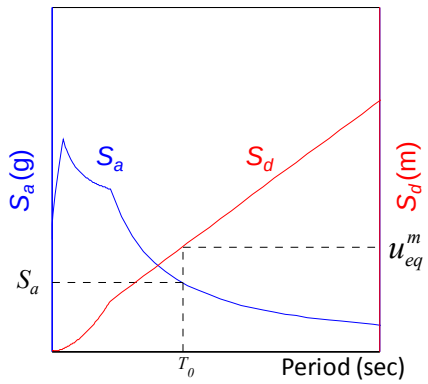

Fig. 6 Nonlinear displacement and acceleration spectra

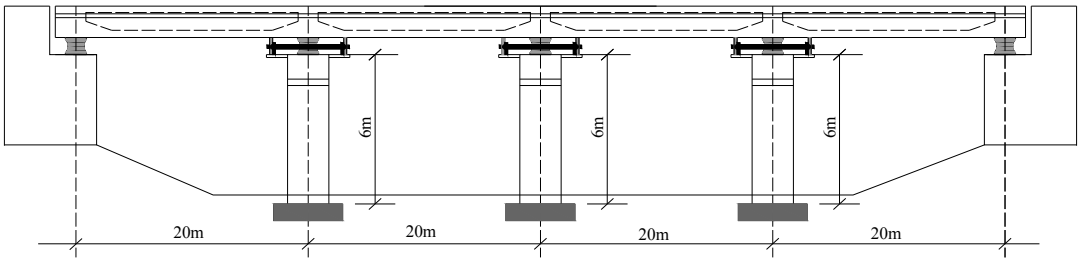

Fig. 7 A four-span RC highway bridge with SMA base isolators

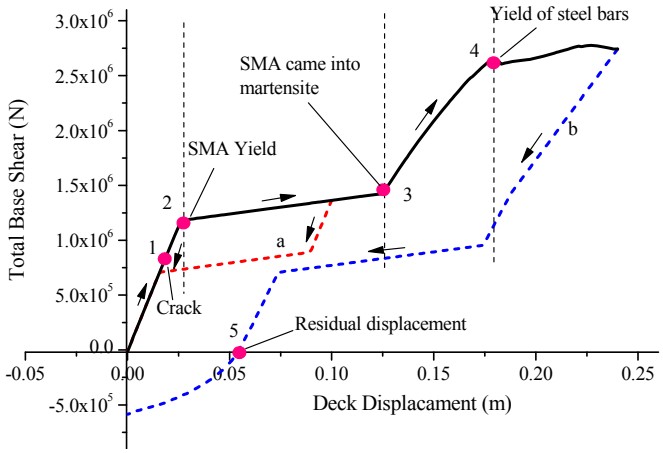

(a) Base shear - deck displacement relationship

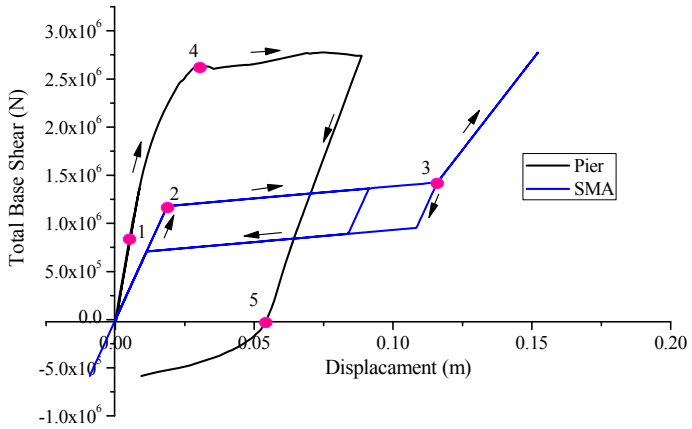

(b) Force-displacement relationship of the SMA isolators and piers

Fig. 8 Pushover analysis results of highway bridges with SMA isolators

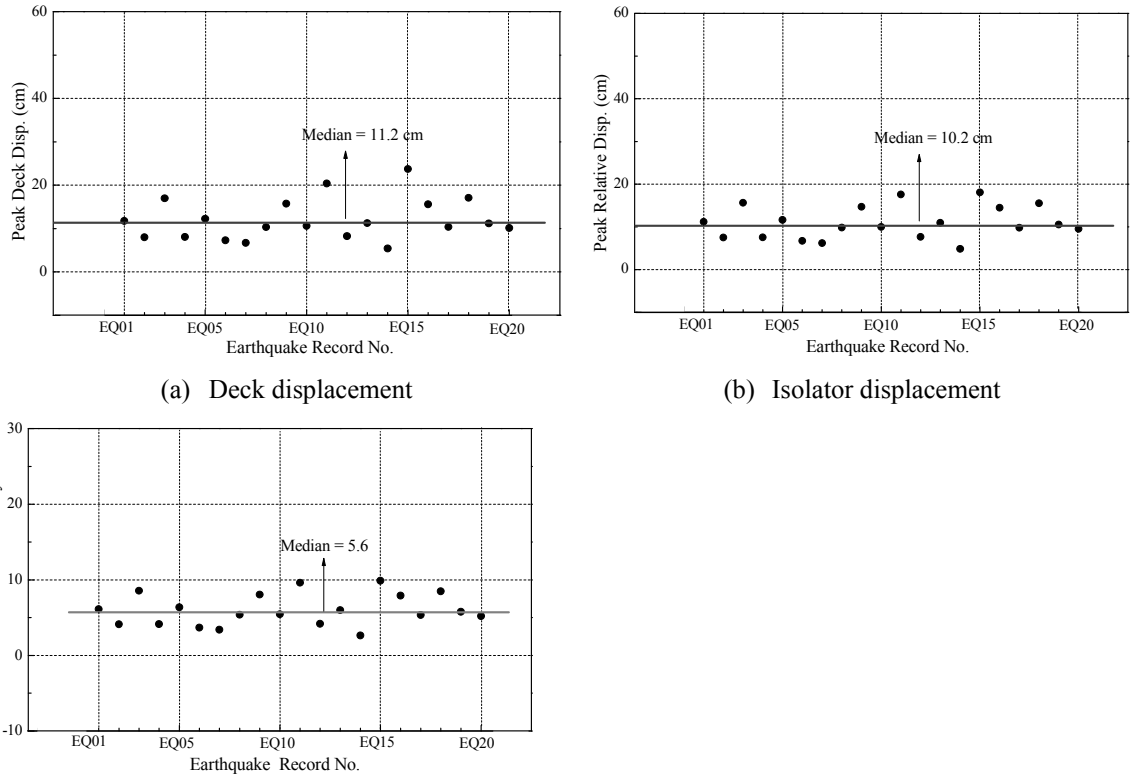

(a) Deck displacement (b) Isolator displacement

(c) SMA ductility

Fig. 9 Peak seismic response under rare earthquakes

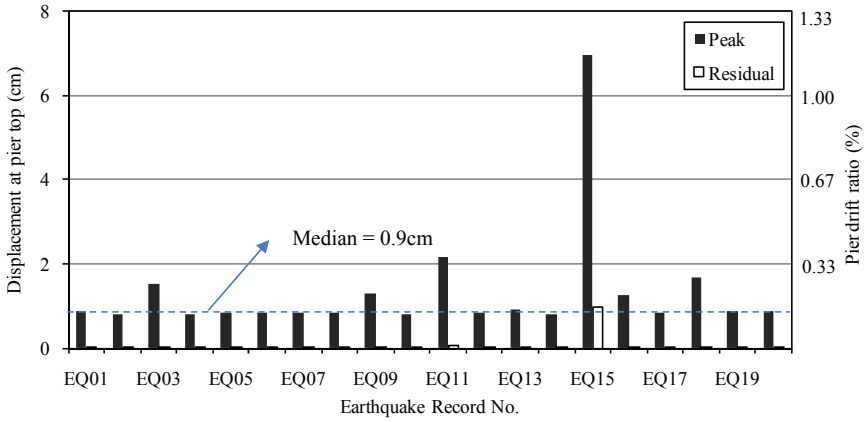

Fig. 10 Peak and residual displacement of the pier top under rare earthquakes

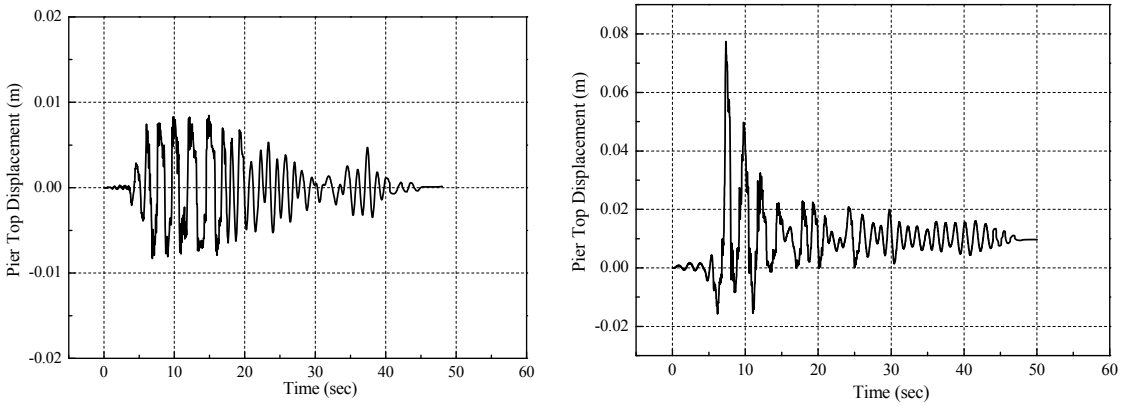

(a) EQ01 (b) EQ15

Fig. 11 Time history of pier top displacement under EQ01 and EQ15

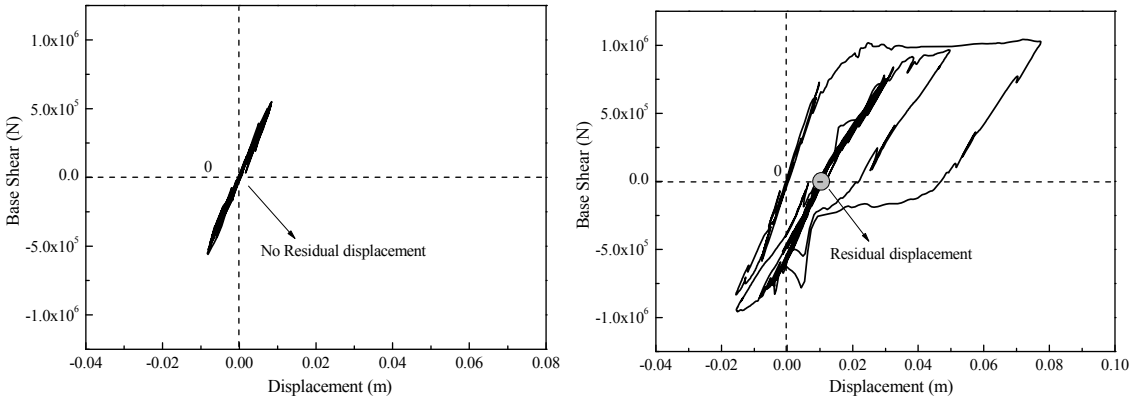

(a) EQ01 (b) EQ15

Fig. 12 Lateral force-displacement relationship of bridge pier under EQ01 and EQ15

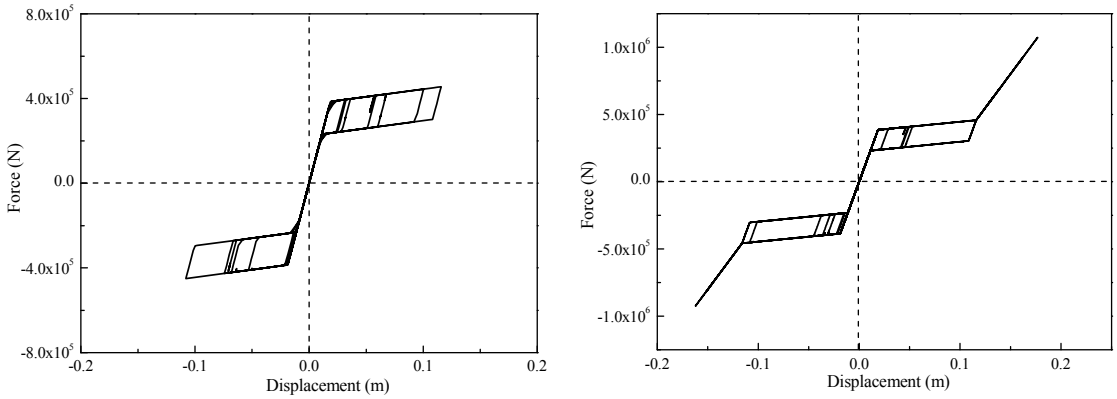

(a) EQ01 (b) EQ15

Fig. 13 Lateral force-displacement relationship of SMA isolator under EQ01 and EQ15

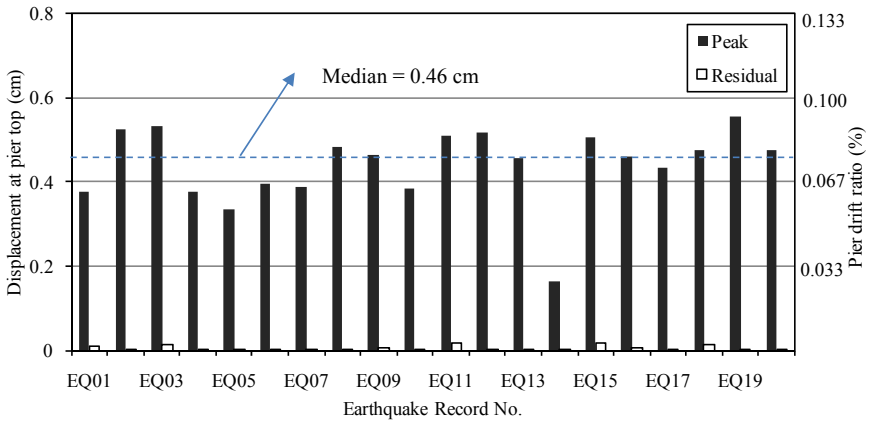

Fig. 14 Peak and residual displacement of the bridge pier under frequent earthquakes